Magnetic coupling in superposed type-II superconducting films[*]

J. W. Ekin[†] and B. Serin[‡]

Physics Department, Rutgers University, New Brunswick, New Jersey 08903

John R. Clem

Ames Laboratory-USAEC and Department of Physics, Iowa State University, Ames, Iowa 50010

A study has been made of the magnetic-coupling properties of vortex arrays in a dc superconducting transformer composed of two oxygen-doped aluminum films separated by a thin insulating layer. By doping to the appropriate level, very small depinning currents have been achieved, making possible an investigation of the vortex-coupling characteristics in a low-current regime free of heating instabilities. Measurements of the system's V-I characteristics have been obtained at currents more than an order of magnitude greater than the current at which the two vortex lattices cease to move at the same velocity. A simple periodic-coupling-force model has been used to generate theoretical V-I curves which are found to compare well with the experimental data. Values of the magnetic interaction force coupling the two vortex arrays have been determined as a function of temperature and intervortex spacing, and are compared with theory.

I. INTRODUCTION

The coupled motion of vortices in two superposed electrically insulated superconducting films was first observed by Giaever[1] in 1965 and subsequently by other investigators.[2-5] In this experiment, two ~ 1000-Å-thick type-II superconducting films sandwich a very thin (~ 200-Å) dielectric layer. An applied perpendicular magnetic field is used to establish in both films an array of Abrikosov microstructures[6] which magnetically couple together through the thin insulating layer. When a current of sufficient magnitude to depin the vortices is passed through one of the films, the vortex lattice in that film is set in motion, inducing a dc voltage along its length. If the magnetic coupling with the superposed secondary vortex lattice is strong enough, it will be dragged along by the motion of the primary vortex lattice and a dc voltage will appear across the secondary film. Thus we have, in effect, a superconducting dc transformer, wherein a dc voltage across the primary film magnetically induces a dc voltage in an electrically insulated secondary.

Attempts to measure the vortex-coupling characteristics of these thin-film systems, however, have repeatedly met with problems of large depinning currents and heating instabilities. Here we report experimental measurements of coupled-vortex behavior in a superconducting granular-aluminum-film system, where depinning currents have been reduced by more than two orders of magnitude over those present in previous experiments. In Sec. II we will discuss the condition that generates the pinning problem in the dc transformer, and in Sec. III we discuss how this problem is overcome by the granular-aluminum system. In Sec. IV measurements of the coupled V-I characteristics will be presented for the granular-aluminum dc transformer and compared with the results of a relatively simple periodic-coupling-force model. Finally, in Sec. V some of the properties of this coupling force will be determined from the measured V-I characteristics and compared with the results of a Gibbs-free-energy calculation of primary-secondary vortex interaction.

II. HEATING INSTABILITIES AND PREVIOUS MEASUREMENTS

In previous experiments on the dc-transformer system, the superconducting layers were made of tin[1-4] or an indium-lead alloy,[5] and in these materials large currents (typically hundreds of milliamperes) were essential in order to depin the vortices. The high depinning currents were the result of the low magnetic field strengths at which the experiments must be performed. In particular, the interaction potential coupling the two vortex lattices arises from the spatial modulation of the magnetic field seen by the lattice in one film due to the vortex structure in the other (see Fig. 1). When the vortex spacing becomes comparable to the thickness d_i of the dielectric layer, spreading of the magnetic field lines within the dielectric region seriously degrades the modulation profile and the coupling strength rapidly diminishes. Strong coupling occurs only when

$$g_{10}d_i \ll 1, \tag{1}$$

where g_{10} is the shortest reciprocal-lattice vector for the triangular vortex lattice, $g_{10} = (8\pi^2 B/\sqrt{3}\phi_0)^{1/2}$, with B the magnetic induction and ϕ_0 the flux quan-
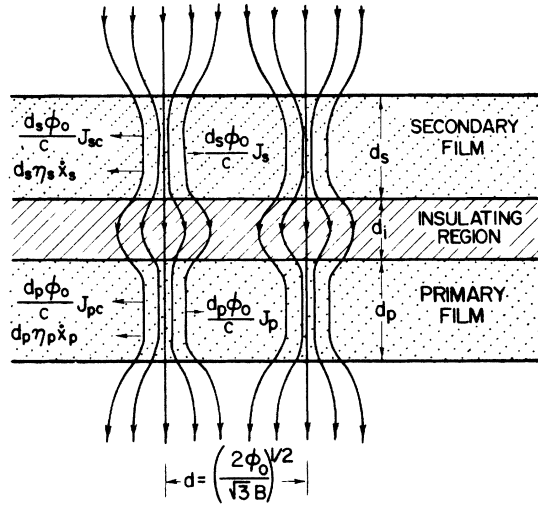
FIG. 1. Schematic representation of the forces and magnetic fields associated with the two vortex arrays (shown in register).

tum, $\phi_0 = hc/2e$. This condition in practice necessitates magnetic field strengths as low as 10 G or less.[7]

Because of the large depinning thresholds in most materials under these low-field conditions, coupled-vortex motion has been previously observed only at high current densities where heating-instability problems occur. In such investigations, the applied primary current would typically drive the primary film normal, causing its resistance to jump to its normal-state value. The Joule heating of the primary would in turn drive the secondary normal, causing the secondary voltage to drop abruptly to zero (in the absence of applied secondary current). Thus heating instabilities and large pinning forces dominated the decoupling characteristics. In an effort to overcome these problems and experimentally study the force coupling the two vortex arrays, we have turned to a granular-aluminum-film system.

III. SAMPLE PREPARATION AND EXPERIMENTAL PROCEDURE

Anomalously small depinning thresholds can be obtained in granular-aluminum films under certain conditions. These films are prepared by evaporating aluminum in the presence of a partial pressure of oxygen,[8] which has the effect of greatly reducing the average aluminum grain size occurring in these films.[9] As the level of oxygen doping is increased, eventually the temperature-dependent coherence length (and hence the vortex-core size) will also be reduced. But for a certain intermediate level, corresponding to a normal-state resistivity of about 10 $\mu\Omega$ cm, the vortex-core size can

be made large compared to the scale of structural disorder (see Fig. 2). Aluminum films with oxygen-doping levels in this intermediate regime are observed to have the lowest depinning currents.[10]

The results reported here were obtained in a dc-transformer system composed of two 740-Å-thick granular-aluminum films separated by a 120-Å SiO insulating layer (isolation resistance greater than 10^7 Ω). The aluminum films were prepared by evaporating high-purity (99.999%) aluminum in a partial pressure of oxygen onto a room-temperature substrate made of fire-polished Corning 7059 glass. The glass substrate was placed approximately 14 cm from the evaporation source and the evaporation was carried out at a constant oxygen pressure of $\sim 1 \times 10^{-5}$ Torr and deposition rate of from 5 to 10 Å/sec. This combination produced aluminum films with normal-state-resistivities at 4.2 °K in the desired 10 $\mu\Omega$ cm range.

Each film was deposited in a conventional four-lead configuration allowing measurement of the voltage-current characteristic of the superposed portion (see Fig. 3). Both films were constructed to be of equal width, and coupled-vortex motion was achieved using either film as primary.

IV. V-I CHARACTERISTICS

The electric field $\vec{E}$ arising from the steady-state motion of flux lines in a type-II superconducting film is given by the usual expression[11]:

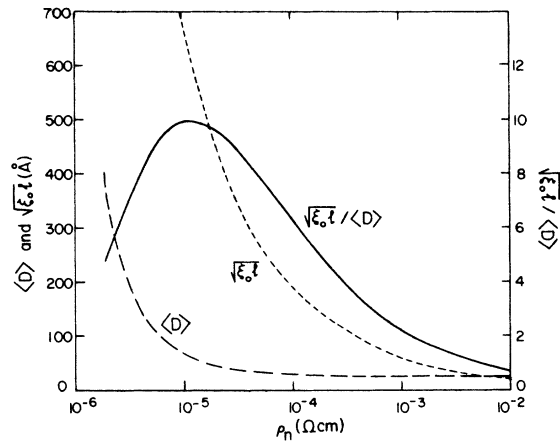$$\vec{E} = -c^{-1}\vec{x} \times \vec{B}, \qquad (2)$$

FIG. 2. Average grain size $\langle D \rangle$ (long-dashed curve), $(\xi_0 l)^{1/2}$ (short-dashed curve), and ratio of the two (solid curve) determined as a function of the normal-state resistivity ρ_n. The electronic mean free path l was obtained from $\rho_n l = 0.4 \times 10^{-11}$ Ω cm^2, $\langle D \rangle$ from Fig. 8 of Ref. 9, and ξ_0 from the pure-aluminum BCS coherence length (16000 Å) multiplied by the ratio of T_c for pure aluminum (1.19 °K) to T_c for the granular film (also a function of ρ_n, Ref. 9).
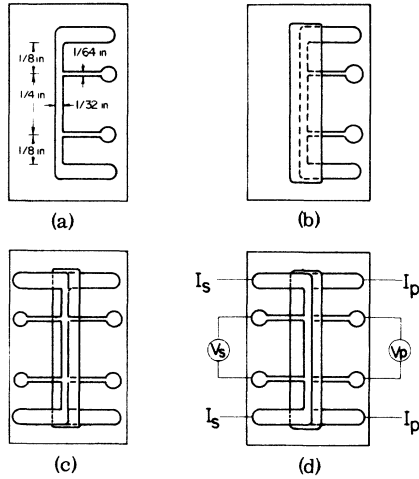
FIG. 3. Configuration of the dc transformer used in this work: (a) primary granular aluminum film, (b) SiO insulating layer, (c) secondary granular aluminum film, (d) voltmeter and current-source connections.

where $\vec{x}$ is the flux-flow velocity. Using this relationship, the dc voltage induced along the length of either film can be used as a measure of time-averaged motion of vortex lines in that film.

A typical set of V-I characteristics is presented in Fig. 4, where both primary and secondary voltages have been plotted as a function of applied primary current at several fixed values of the perpendicular magnetic field H. (Because of the large demagnetization coefficient in this thin-film geometry, H is equal to the magnetic induction B.) Focusing on one pair of curves, it will be seen that both primary and secondary voltages initially rise together as the primary current is increased above the depinning threshold. In this perfect-coupling regime the motion of the vortex lines in the secondary is coincident with that of the primary, due to the attractive magnetic interaction through the dielectric layer, which tends to keep the two vortex lattices in register. However, as the primary current is increased, eventually the viscous-drag force acting on the secondary vortex lattice, combined with the secondary pinning force, exceeds the maximum coupling force. At this point perfect coupling breaks down. Slippage occurs between the two vortex arrays and the primary voltage begins to increase at a faster rate with current, whereas the secondary voltage decreases. This behavior indicates the onset of dynamic coupling.

We now quantitatively interpret these results in terms of a model originally proposed by Cladis, Parks, and Daniels,[5] which we have extended to include the important effects of pinning. As described in the preceding paper,[12] we consider a

model involving (see Fig. 1) a Lorentz force due to the applied current, a pinning force for the individual lattices, a viscous-drag force proportional to the speed $\dot{x}$, and a periodic-coupling force which we take to have a simple sinusoidal form, as justified in Ref. 12. The coupling force experienced by the primary is equal and opposite to that felt by the secondary, thus resulting in a coupled pair of equations of motion:

Viscous drag force	net force from = applied current + and pinning	periodic coupling force
$d_p \eta_p \dot{x}_p$ =	F_p	$- F_m \sin[(2\pi/d)(x_p - x_s)]$,

$$\qquad\qquad (3a)$$

$d_s \eta_s \dot{x}_s$ =	F_s	$+ F_m \sin[(2\pi/d)(x_p - x_s)]$.

$$\qquad\qquad (3b)$$

Here d is the vortex spacing in the direction of flow $[d = 4\pi/g_{10}\sqrt{3} = (2\phi_0/B\sqrt{3})^{1/2}]$, x_p and x_s represent the position coordinates of the primary- (p) and secondary- (s) vortex lattices (assumed rigid), η_p and η_s are the viscous-drag coefficients for the primary and secondary films, and d_p and d_s are the corresponding film thicknesses.

Within the primary film, the net force arising from the applied current and pinning can be given more explicitly as

$$F_p = (J_p \mp J_{pc})\, \phi_0 d_p/c, \qquad\qquad (4)$$

where J_p is the applied current density and J_{pc} is the depinning-critical-current density [the negative (positive) sign holds for coupled-vortex motion in the same (opposite) direction as the Lorentz force due to the applied current]. A similar expression with the subscript p replaced by s holds for the secondary film. Upon substituting Eqs. (2) and (4) into Eq. (3) and reexpressing in terms of each film's flux-flow resistance R, applied current I,
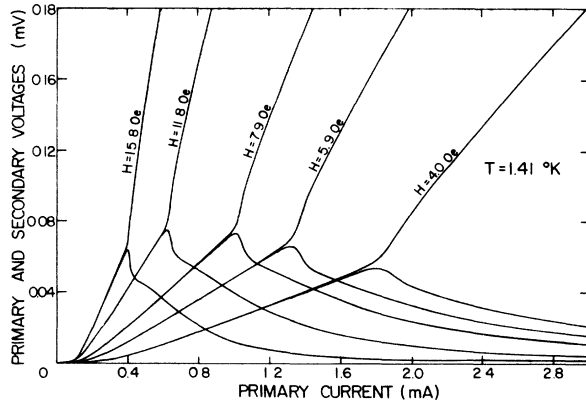

FIG. 4. Primary and secondary voltages as a function of applied primary current for several magnetic field strengths (zero applied secondary current).
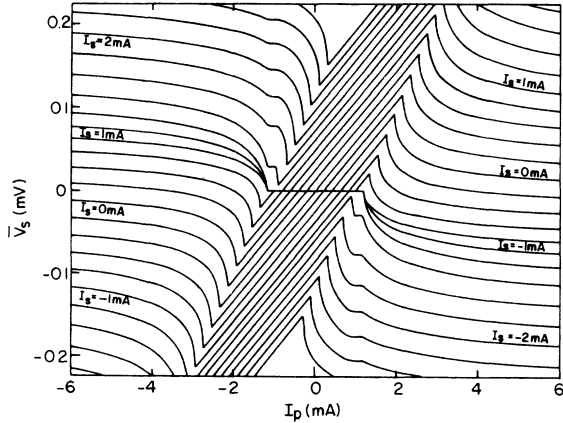
FIG. 5. Theoretical plot of the average secondary voltage $\bar{V}_s$ vs primary current I_p at a series of values of secondary current I_s. The curves were generated from Eqs. (5) using parameters obtained from the experimental data in Fig. 6 at $T = 1.395\,°K$ and $H = 5.9$ Oe: $R_p = 0.122$ Ω, $R_s = 0.121$ Ω, $I_0 = 1.06$ mA, $I_{pc} = 0.12$ mA, and $I_{sc} = 0.29$ mA.

FIG. 6. Experimental plot of the dc secondary voltage $\bar{V}_s$ vs primary current I_p at a series of values of secondary current I_s. Data were obtained at $T = 1.395\,°K$ and $H = 5.9$ Oe with the bottom film used as primary; sample parameters are presented in Table I.

critical depinning current I_c, and voltage V, we have [corresponding to Eqs. (3.3) and (3.4) of Ref. 12]

$$V_p = (I_p \mp I_{pc}) - I_0 \sin\frac{2\pi(x_p - x_s)}{d} \, R_p, \qquad (5a)$$

$$V_s = (I_s \mp I_{sc}) + I_0 \sin\frac{2\pi(x_p - x_s)}{d} \, R_s. \qquad (5b)$$

Here I_0 is related to the maximum coupling force F_m by

$$F_m = \phi_0 I_0/cw, \qquad (6)$$

where w is the width of the film. Equations (5) determine the coupled V-I characteristics of the system in terms of the five parameters R_p, R_s, I_{pc}, I_{sc}, and I_0. We have solved the system of equations and present a typical set of V-I characteristics in Fig. 5.

This figure is to be compared with the experimentally measured V-I characteristics presented in Fig. 6. (The parameters for this particular sample have been listed in Table I; eight other samples were also investigated with qualitatively similar results to those described here.) As far as the general configuration of the V-I characteristics is concerned, the experimental curves and the calculated results of this relatively simple model are in excellent over-all agreement with each other. Using parameters R_p, R_s, I_c, I_{pc}, and I_{sc} determined from the data in the upper half-plane of Fig. 6, the theoretical results in Fig. 5 exhibited maximum deviations from the experimental curves of less than 0.02 mV over the entire range of applied currents. [13] (Similar results, not
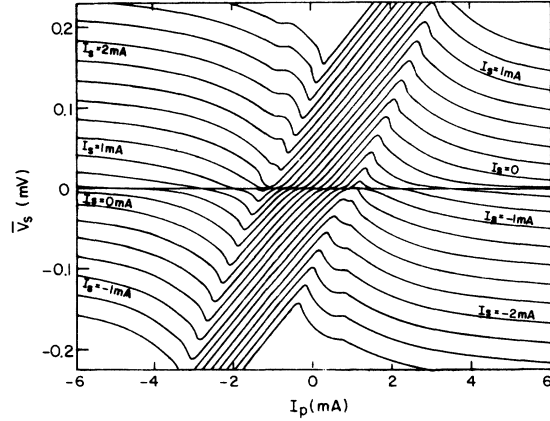
shown, were obtained for the primary V-I characteristics.) Note that even the series of small plateaus appearing in the upper left-hand and lower right-hand quadrants of the experimental plot are well accounted for in the theoretical curves. These are a result of pinning of the primary vortex lattice during a portion of the phase-slip cycle. [14]

A slight shifting of the experimental and theoretical curves, however, can be noticed at negative voltages upon detailed comparison of Figs. 5 and 6. Since the five parameters used in generating the theoretical curves of Fig. 5 had been determined from the experimental data in the upper half-plane of Fig. 6 (positive voltages) a separate determination of the parameters was performed from the negative-voltage data. This yielded the same values of R_p, R_s, and I_0 within experimental error as for positive voltages, but the critical depinning currents, I_{pc} and I_{sc}, were found to be significantly different. The motion of the vortices is in opposite directions for the two cases, thus indicating anisotropy in the pinning. In particular, it suggests that edge-pinning effects may be playing a role, which seems quite reasonable in an experiment such as this where bulk pinning has been greatly reduced.

Such effects, however, are small and easily provided for in terms of the model considered here by using different critical currents in the two regimes. Over-all, the periodic-coupling-force model expressed by Eqs. (5) provides a simple accurate description of these experimental data.

V. COUPLING FORCE

The model presented above can be used to determine from the measured V-I characteristics

TABLE I. Parameters characterizing the dc trans-
former used in this work.

	Primary	Secondary
Film thickness	$d_p = 740$ Å	$d_s = 740$ Å
Normal resistivity	$\rho_{np} = 8.34\ \mu\Omega$ cm	$\rho_{ns} = 9.03\ \mu\Omega$ cm
Electronic mean free path[a]	$l_p = 48$ Å	$l_s = 44$ Å
Transition temperature	$T_{cp} = 1.5$ °K	$T_{cs} = 1.5$ °K
BCS coherence length[b]	$\xi_{0p} = 12\,500$ Å	$\xi_{0s} = 12\,500$ Å
Mean grain size[c]	$\langle D \rangle_p = 80$ Å	$\langle D \rangle_s = 75$ Å
Dielectric layer thickness		$d_i = 120$ Å

[a]Determined from the normal-state resistivity at 4 °K
using $\rho_n l = 0.4 \times 10^{-11}\ \Omega\,cm^2$ [T. E. Faber and A. B. Pip-
pard, Proc. R. Soc. A 231, 336 (1955)].

[b]Determined from the pure-aluminum coherence length
(16000 Å) by multiplying by the critical temperature for
pure aluminum (1.19 °K) and dividing by T_c for the gran-
ular films.

[c]From Ref. 8; see Fig. 2 of this paper.

some of the properties of the magnetic interaction
force coupling the two vortex arrays. Here we
make a preliminary examination of the absolute
magnitude of the maximum coupling force and its
dependence on temperature and magnetic field.

Values of the maximum coupling force F_m have
been obtained by taking a complete set of V_s-I_p-
I_s characteristics (as in Fig. 6) at a series of
temperature and magnetic field values. A fit to
each set of characteristics was made using the
five parameters of Eqs. (5), and F_m was then de-
termined from I_0 using Eq. (6). [15]

The temperature dependence of the results for
F_m is presented in Fig. 7. For the case where
the penetration depth λ is large compared with the
intervortex spacing, the Gibbs-free-energy cal-
culation described in the preceding paper predicts
that the temperature dependence of F_m should vary
as λ^{-4}. [16] With this in mind we have attempted to
fit the data of Fig. 7 to a temperature-dependent
form given by

$$F_m = \beta[1 - (T/T_c)]^2 , \qquad (7)$$

where T_c is the experimentally measured transi-
tion temperature, 1.515 °K. The results of the
fit are shown by solid curves in Fig. 7, the ex-
perimental data points by circles. As is evident
from the figure, the temperature dependence of
the maximum coupling force F_m is well described
by this theoretical form.

The absolute magnitude and magnetic field de-
pendence of the maximum coupling force are also
shown in Fig. 7, where values of the single pa-
rameter β used in fitting the experimental data are
plotted as a function of inverse field H^{-1}. In ac-
cordance with the discussion in Sec. III, the mag-
nitude of β decreases with increasing magnetic
field, due to the decrease in field modulation pro-
file at higher vortex densities. A precise evalua-
tion of the Gibbs-free-energy results for the mag-

nitude and magnetic field dependence of β has not
yet been completed, but we can nevertheless com-
pare these experimental results with an approxi-
mate evaluation of the coupling-force magnitude
calculated in the one-reciprocal-lattice-vector
approximation. [12] In this simplifying approximation
the maximum coupling force F_m is given by[17]

$$F_m = \frac{3\phi_0^2 d_p d_s}{32\pi^3 \lambda_p^2 \lambda_s^2} \tilde{F}_m , \qquad (8)$$

where λ_p (λ_s) is the penetration depth for the pri-
mary (secondary) film:

$$\lambda_p = 0.64\lambda_L(0)\ (\xi_{0p}/l_p)^{1/2}\ [1 - (T/T_c)]^{-1/2} \qquad (9)$$

(with l_p, ξ_{0p}, and λ_L the primary's electronic mean
free path, BCS coherence length, and zero-tem-
perature London penetration depth, respectively).
$\tilde{F}_m$ is a dimensionless magnetic-field-dependent
factor, which for the magnetic field strengths used
here is less than, but of the order of, unity:

$$\tilde{F}_m = e^{-\tilde{g}\ d_i/d_f}\ (1 - e^{-\tilde{g}})^2/\tilde{g}^2 \qquad (10)$$

(here we have assumed the primary and secondary
films to be of equal thickness d_f; $\tilde{g} \equiv g_{10} d_f$). Eval-
uating Eq. (8) using the sample parameters given
in Table I, [18] we find the calculated magnitude of
the coupling-force parameter β to be

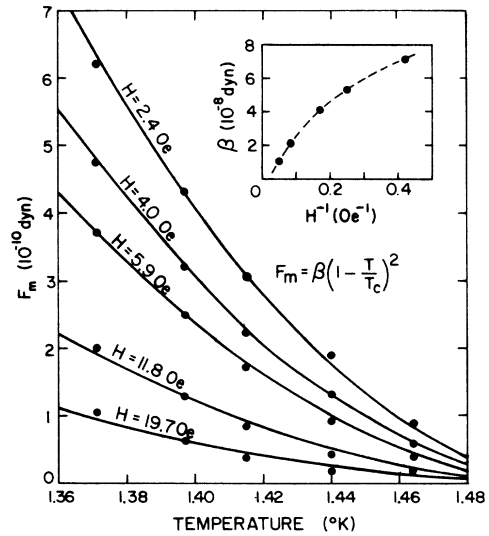$$\beta = 9.5 \times 10^{-8}\ \tilde{F}_m\ \text{dyn.} \qquad (11)$$

FIG. 7. Maximum coupling force F_m as a function of
absolute temperature T for a series of values of the mag-
netic field H. Circles—experimental data. Solid curves—
fit to the temperature-dependent form $F_m = \beta(1 - T/T_c)^2$;
values determined for the coupling-force parameter β
are shown in the insert. The transition temperature T_c
for the sample was measured to be 1.515 °K; other sam-
ple parameters are presented in Table I.

This agrees well with the magnitude of the experimental results for β in Fig. 7.

In summary, it has been possible to investigate the magnetic coupling of superposed vortex arrays under conditions of reduced pinning and negligible Joule heating, through the use of granular aluminum films in which the coherence-length-to-grain-size ratio has been optimized. V-I characteristics for the dc-transformer system have been measured both in the region of perfect coupling, where the motion of the primary and secondary fluxoids is coincident, and in the region of dynamic coupling, where slippage occurs between the two vortex arrays. Over the entire range of coupling conditions, the V-I characteristics are found to be accurately described by a relatively simple periodic-coupling-force model. This model has in turn been used to determine from the experimental data some of the properties of the magnetic force coupling the superposed vortex arrays. In particular, the temperature dependence, magnetic field dependence, and absolute value of the coupling force have been measured; the data are found to agree well in over-all magnitude and temperature dependence with the results of a Gibbs-free-energy calculation describing the magnetic interaction of the two vortex arrays.

ACKNOWLEDGMENTS

*Research supported by the National Science Foundation.

†Present address: Cryogenics Division, Institute for Basic Standards, National Bureau of Standards, Boulder, Colo. 80302.

‡Present address: University of Manchester, Institute of Science and Technology, Manchester M60 1QD, United Kingdom.

[1]I. Giaever, Phys. Rev. Lett. 15, 825 (1965).

[2]I. Giaever, Phys. Rev. Lett. 16, 460 (1966).

[3]R. Deltour and M. Tinkham, Phys. Rev. 174, 478 (1968).

[4]P. E. Cladis, Phys. Rev. Lett. 21, 1238 (1968).

[5]P. E. Cladis, R. D. Parks, and J. M. Daniels, Phys. Rev. Lett. 21, 1521 (1968).

[6]A. A. Abrikosov, Zh. Eksp. Teor. Fiz. 32, 1442 (1957) [Sov. Phys.-JETP 5, 1174 (1957)].

[7]For example, at a typical dielectric layer thicknesses d_i of 118 Å, and a magnetic field of 10 G, $g_{10}d_i = 0.35$.

[8]B. Abeles, R. W. Cohen, and G. W. Callen, Phys. Rev. Lett. 17, 632 (1966); B. Abeles, R. W. Cohen, and R. W. Stowell, Phys. Rev. Lett. 18, 902 (1967); R. W. Cohen and B. Abeles, Phys. Rev. 168, 444 (1968).

[9]G. Deutscher, H. Fenichel, M. Gershenson, E. Grünbaum, and Z. Ovadyahu, J. Low Temp. Phys. 10, 231 (1973).

[10]J. W. Ekin (unpublished data).

[11]See, for example, Y. B. Kim and M. J. Stephen, in Superconductivity, edited by R. D. Parks (Marcel Dekker, New York, 1969), Chap. 19.

[12]John R. Clem, preceding paper, Phys. Rev. B 9, 898 (1974).

[13]The rounding of the peaks is believed to be a result of film inhomogeneities introduced by evaporation-rate fluctuations in preparing the samples.

[14]See, for example, Fig. 5 of Ref. 12.

[15]Note that edge-pinning effects discussed in Sec. IV do not interfere with the determination of I_0, provided the fit is made to the V-I characteristics in either the upper or lower half-plane, where vortex motion is consistently in one direction.

[16]See Eqs. (2.6) and (2.7) of Ref. 12. Note that this form for the temperature dependence of F_m is not dependent on the one-reciprocal-lattice-vector approximation discussed in Ref. 12, but holds generally for the large-penetration-depth case.

[17]See Eq. (2.24) of Ref. 12.

[18]The zero-temperature London penetration depth λ_L for these films was taken to be the pure-aluminum value of 157 Å.